

Received: 14 December 2022

Revised: 19 January 2023

Accepted: 19 January 2023

Characterization of triglycerides photooxidation under solar radiations: A stepwise Raman study

Ali Assi¹  | Rime Michael-Jubeli¹ | Carine Jacques-Jamin² | Arlette Baillet-Guffroy¹ | H el ene Duplan² | Ali Tfayli¹

¹Lipides: Syst emes Analytiques et Biologiques, Lip(Sys)2, Faculty of Pharmacy, Universit e Paris-Saclay, Orsay, France

²Center of Research Pierre Fabre Dermo-Cosmetics (PFDC), Toulouse, France

Correspondence

Ali Tfayli, Lipides: Syst emes Analytiques et biologiques, Lip(Sys)2, Faculty of Pharmacy, Universit e Paris-Saclay, Orsay, France.
Email: ali.tfayli@universite-paris-saclay.fr

Abstract

Triglycerides (TGs) are one of the main components of the glycerolipid family. Their main task in cells is to store excess fatty acids. TG energy storage is mainly concentrated in adipocytes. TGs and free fatty acids constitute the majority (57.5%) of the skin surface lipids (SSLs). TGs are essential for the formation of the skin water barrier. This work is the second part of a global study that aims to evaluate the effect of solar radiations on SSLs using vibrational spectroscopy. In the first part of this work, a stepwise characterization of free fatty acids was performed, and different spectral descriptors were used to follow the different structural modifications during the photo-oxidation process, that is hydrogen abstraction, formation of hydroperoxides and peroxy radicals as primary oxidation products and the formation of aldehydes, ketones, alcohol as secondary products. In this second part, the photo-oxidation of TGs was evaluated using Raman spectroscopy. A decrease in the CH_2/CH_3 stretching bands ratio that confirmed the hydrogen abstraction, an increase in the $1165/1740\text{ cm}^{-1}$ ($\delta(\text{OH})$ and $\nu(\text{C}-\text{O})/\nu(\text{C}=\text{O})$ (ester)) ratio indicated the formation of secondary oxidation products such as hydroperoxides. And finally, an increase in the $1725/1740\text{ cm}^{-1}$ ($\nu(\text{C}=\text{O})$ (ald.)/ $\nu(\text{C}=\text{O})$ (ester)) ratio and the *trans* $\nu(\text{C}=\text{C})$ /*cis* $\nu(\text{C}=\text{C})$ ratio highlighted the formation of aldehydes, alcohols, ketone, *trans* secondary products and others.

KEYWORDS

lipid Peroxidation, malondialdehyde, skin surface lipids, solar radiations, triglycerides, vibrational spectroscopy

1 | INTRODUCTION

Lipids are heterogeneous biomolecules with many important roles. In humans, lipids can function as energy substrates, steroid hormones, inflammatory mediators, transporters and as structural elements of cellular and organelle membranes.¹

Lipids include eight major classes with distinct chemical properties: fatty acids, glycerolipids, glycerophospholipids, sphingolipids, sterols, prenol, glycolipid and polyketides.^{1,2}

Lipid peroxidation (LPO) is the most studied biologically relevant free radical chain reaction.³ It generates reactive oxygen species (ROS) that oxidize the polyunsaturated lipids, and it is thus considered a critical step in the pathogenesis of several disease states.⁴⁻⁶ In the skin, LPO is mainly related to photooxidation. It induces an alteration in

Abbreviations: LPO, lipid peroxidation; MDA, malondialdehyde; ROS, reactive oxygen species; SSLs, skin surface lipids; TG, triglyceride.

This is an open access article under the terms of the [Creative Commons Attribution-NonCommercial-NoDerivs License](https://creativecommons.org/licenses/by-nc-nd/4.0/), which permits use and distribution in any medium, provided the original work is properly cited, the use is non-commercial and no modifications or adaptations are made.

  2023 The Authors. *Analytical Science Advances* published by Wiley-VCH GmbH.

the barrier function and may lead to skin diseases, such as photoaging, psoriasis, atopy and skin cancer.⁷⁻¹⁰

Thus, the study of changes in the structure of lipids and the analysis of LPO products have received significant attention in recent years in the field of medicine and biology. It has been linked to a wide range of diseases, including cancer,¹¹ cardiovascular diseases¹² and neurodegenerative disorders.^{13,14}

Polyunsaturated lipids with two or more double bonds are more prone to LPO. LPO is initiated by free radicals (ROS) and produces hydroperoxides as primary products. These latter are unstable and decompose rapidly into a variety of aldehyde products as secondary products, especially malondialdehyde (MDA), 4-hydroxy-2-nonenal (HNE), 4-hydroxy-2-hexenal (4-HHE) and other minor products.¹⁵⁻¹⁷

LPO can be produced by auto-oxidation, enzymatic oxidation or photo-oxidation initiated by radiant energy, such as ultraviolet, solar radiations or artificial light.^{5,6,17,18}

Even though solar UVRs are essential to the body such as stimulating the production of vitamin D, they can induce oxidative stress that alters lipid composition. For example, solar UV exposure can reduce FAs and triglycerides (TGs) in the epidermis, which results in skin photoaging.¹⁹

Many methods described in the literature have been used to determine the degree of LPO, including spectrophotometry, high-performance liquid chromatography and gas chromatography coupled to the mass spectrometry.²⁰⁻²⁵

In addition, vibrational spectroscopy has also been used to characterize LPO products.^{17,26-29} Vibrational techniques are well suited for use with biological samples as they provide highly specific, molecular-level information without the need for significant sample preparation or large sample volumes.³⁰ More specifically, Raman spectroscopy can operate in aqueous environments and can be directly used in situ.³¹

In the first part of this study, vibrational spectroscopy was used to evaluate modifications in FFAs during the oxidation process, including saturated and unsaturated types with various double bonds and chain lengths. Raman descriptors were used to track the formation of hydroperoxides, alcohols, and fragmentation of alkyl chains, and IR spectroscopy was used to confirm the formation of hydroperoxides and secondary oxidation products such as aldehydes.¹⁷

In this part, the effect of solar radiations on TGs was investigated. TGs are one of the main components of the glycerolipid family.³² They are the major metabolic energy and fatty acid storage molecules in most organisms.³³ TGs are a heterogeneous group of molecules with a glycerol backbone and three FAs linked by ester bonds. Their physical and chemical properties differ depending on the chain length and degree of unsaturation of their FAs.³³

TGs serve multiple important functions in living organisms. Due to their highly anhydrous property, TGs are the primary storage molecules of FAs for energy utilization and the synthesis of membrane lipids. TGs in plants are the main constituent of seed oils and are an important resource in food consumption and industrial uses. Moreover, they can be used for biofuels.³³

In animals, the energy storage of TG is mainly concentrated in adipocytes. In addition to their role in storing energy, TG synthesis in

cells protects them from the potentially toxic effects of excess FAs. Although TGs are essential for normal physiology, an excessive accumulation of TGs in human adipose tissue contributes to obesity and is associated with organ dysfunction in non-adipose tissue.³³

TGs and free fatty acids constitute the largest part of the skin surface lipids (SSLs) (57.5%). TGs are essential for the formation of the skin water barrier³⁴ and act as a mechanical cushion around joints and internal organs, and collections of TG in adipose tissue provide insulation for organisms.³³

The aim of this paper was to monitor and evaluate the modifications and changes that may take place after solar irradiation on TGs using Raman spectroscopy. Saturated and unsaturated TGs with different numbers of double bonds and different chain lengths were used.

2 | MATERIALS AND METHODS

2.1 | Chemicals

Tripalmitolein, 1,2-palmitolein-3-palmitin, 1,2-palmitin-3-palmitolein, trilinolein and trilinolenin (Table 1) were purchased from Laro-dan (Solna, Sweden). Chloroform was purchased from Carlo Erba (Chaussée du Vexin, Val-de-Reuil, France). Lipid films are prepared by dissolving fatty acids in chloroform to obtain solutions of 2 mg/mL concentration. Each solution of 20 μ L was deposited on CaF₂ slides. The lipid films were then dried to remove residual solvent traces.

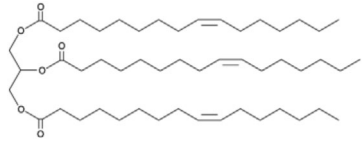
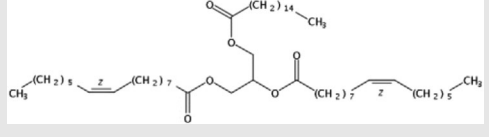
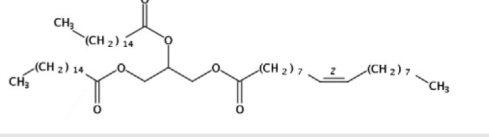
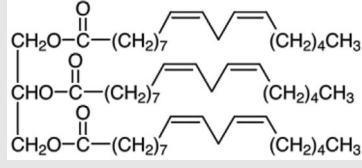
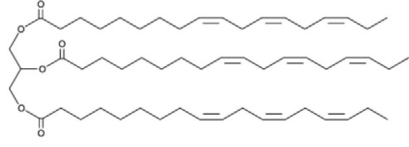
2.2 | Samples irradiation

The five TG were irradiated at different times using a solar simulator 16S-300 (Solar Light, Glenside, PA, USA) which produces a spectrum close to the solar spectrum. The power used for the irradiation was 0.45 W/cm². This power was measured using a pyranometer (Glenside, PA, USA). Table 2 shows the different energies used during the irradiation process.

2.3 | Raman spectroscopy

Raman spectral acquisitions were performed with an HR LabRAM microspectrometer (Horiba scientific, Palaiseau, France). The excitation source is a 633-nm single-mode diode laser (TOPTICA Photonics, Germany) with 35 mW laser power on the sample. The microspectrometer is equipped with an Olympus microscope, and measurements were recorded using a \times 100 MPlan objective (Olympus, Japan). Light scattered by the sample is collected through the same objective. A Peltier-cooled (-65°C) multichannel-coupled charge device detector (1024 \times 256 pixels) detects the Raman Stokes signal dispersed with a 400- μ m slit width and a 600 grooves/mm holographic grating enabling a spectral resolution of 2 cm⁻¹. A calibration procedure was applied daily prior to data collection as recommended by Horiba Scientific. The zero-order position and the laser line were daily checked. Raman

TABLE 1 The 5 triglycerides used in this study lipid

| | | | |
|-----|----------------------------|---------------------|---|
| TG1 | Tripalmitolein | (C16:1/C16:1/C16:1) |  |
| TG2 | 1,2-Palmitolein-3-palmitin | (C16:1/C16:1/C16:0) |  |
| TG3 | 1,2-Palmitin-3-palmitolein | (C16:0/C16:0/C16:1) |  |
| TG4 | Trilinolein | (C18:2/C18:2/C18:2) |  |
| TG5 | Trilinolenin | (C18:3/C18:3/C18:3) |  |

Abbreviation: TG, triglyceride.

TABLE 2 The different solar radiations doses applied to triglyceride (TG) during irradiation in J/cm²

| Time (min) | 2.5 | 5 | 10 | 20 | 40 | 60 | 90 | 120 | 180 | 240 |
|--|---------|--------|--------|--------|---------|---------|---------|---------|---------|---------|
| Total solar spectrum energy (J/cm ²) | 67.5 | 135 | 270 | 540 | 1080 | 1620 | 2430 | 3240 | 4860 | 6480 |
| UV-B energy (J/cm ²) | 0.225 | 0.45 | 0.9 | 1.8 | 3.6 | 5.4 | 8.1 | 10.8 | 16.2 | 21.6 |
| Minimal erythemal dose | 7.5 MED | 15 MED | 30 MED | 60 MED | 120 MED | 180 MED | 270 MED | 360 MED | 540 MED | 720 MED |

relative shift was checked on silica wafer band at 521 cm⁻¹. For the study, the selected spectral range was 400–3800 cm⁻¹. The acquisition of each spectrum required 3 min. Spectral acquisition was performed using LabSpec6 software (Horiba Jobin Yvon SAS, Lille, France).

2.4 | Data analysis

Raman data were analysed with a software developed in-house that operates in the Matlab environment (The MatWorks, Inc., Natick, MA, USA). The background, due to the fluorescence, was corrected using a polynomial function with a polynomial order of 4.³⁵ All spectra were smoothed using the Savitzky–Golay filter on nine points with a polynomial order of 4 and normalized to the AUC of the CH stretching band. Automatic determination of the peak positions was performed using second derivatives.

3 | RESULTS AND DISCUSSION

3.1 | Solar radiations effects on tripalmitolein, 1,2-palmitolein-3-palmitin and 1,2-palmitin-3-palmitolein

TGs are tri-esters consisting of a glycerol bound to three fatty acid molecules. Hence, the oxidation takes place on the fatty acids chain as the ester function remains intact during the oxidation process.²⁶

As explained in the introduction, only the polyunsaturated fatty acids with two or more double bonds are prone to oxidation. Saturated and monounsaturated fatty acids are less vulnerable to LPO.^{17,36}

As expected, no LPO-related modification was observed in the Raman spectra of tripalmitolein (TG1), 1,2-palmitolein-3-palmitin (TG2) and 1,2-palmitin-3-palmitolein (TG3) after applied doses up to 6480 J/cm² (data not shown).

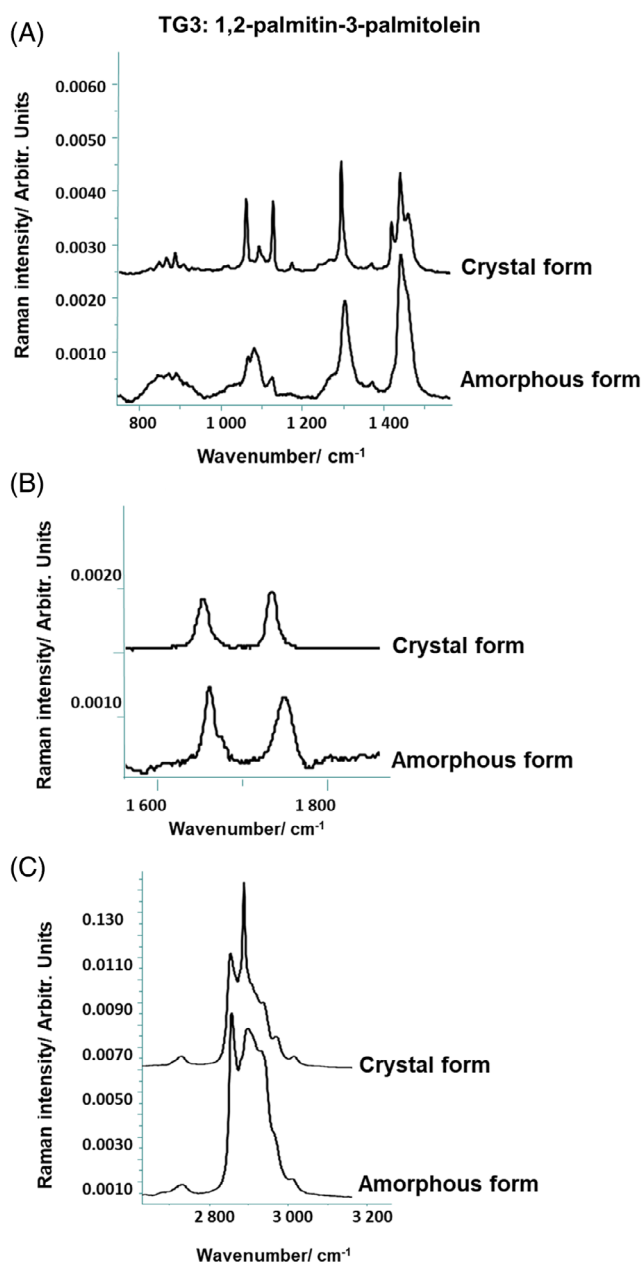


FIGURE 1 Raman spectra of Crystal and amorphous forms of 1,2-palmitin-3-palmitolein (TG3). (A) 750–1470 cm^{-1} region, (B) 1550–1850 cm^{-1} region and (C) 2700–3200 cm^{-1} region.

In addition to oxidation descriptors, conformational order and lateral packing descriptors were also monitored. No significant variations of the *trans/gauche* ratio of the C–C stretching bond and of the $\nu(\text{CH}_2)$ asym/ $\nu(\text{CH}_2)$ sym ratio were noticed for the TG1 and TG2 during the irradiation (data not shown).

For TG3 (1,2-palmitin-3-palmitolein), a change in the state was observed during irradiation (crystal to amorphous). This change was more associated with heating under solar radiations rather than photooxidation.

The spectra of both crystal and amorphous states are presented in Figure 1. For crystal form, the 2800–3000 cm^{-1} region was dominated

by the CH_2 symmetric stretching at about 2880 cm^{-1} . This indicated the presence of a high density of *trans* conformers. For the amorphous form, this band disappeared, and a broadening in the 2800–3000 cm^{-1} region was observed revealing an increase of the *gauche* conformers (Figure 1C).

Same observations were obtained from C–C stretching bands at 900–1150 cm^{-1} . At the crystal state, the region was characterized by sharp peaks and dominated by *trans* conformers (at ~ 1065 and ~ 1130 cm^{-1}), whereas the amorphous form presented a series of overlapping broad bands dominated by a central band at 1080 cm^{-1} (Figure 1A).

In addition to the chain conformational order, the intermolecular chain packing arrangements were affected (Figure 1A). The doublet at ~ 1440 and ~ 1470 cm^{-1} were used as a marker of the presence of crystal form. Moreover, the presence of the factor group splitting band (~ 1420 cm^{-1}) indicated a highly organized orthorhombic perpendicular subcell packing.^{37,38} In amorphous liquid-like state, these bands were replaced by a unique band at almost 1445 cm^{-1} .

The Raman signature of the C=O stretching of the ester was also impacted by the state change with a shift from ~ 1730 cm^{-1} for crystal form to ~ 1750 cm^{-1} for amorphous state.³⁹

The crystal-to-liquid-like state change was observed gradually according to the irradiation time. Indeed, the observation of individual spectra after each cumulative dose revealed an increasing number of TG3 amorphous spectra in the function of the irradiation time. For example, after 10 min of irradiation, the two first spectra corresponded to the amorphous state and seven spectra to the crystal form against 3–6 amorphous to crystal spectra for 20 min. This can be explained by the return to crystal-organized form during spectral acquisition. After 1 h or longer continuous irradiation, the amorphous state remained.

3.2 | Solar radiation effects on trilinolein and trilinolenin

Trilinolein and trilinolenin are homogeneous TGs that contain three identical fatty acids. The former contains fatty acids with double unsaturations and the latter fatty acids with triple unsaturations.

The mechanism of the oxidation of TG with polyunsaturated fatty acids is presented in Figure 2I with the example of trilinolenin oxidation.^{40–45} Figure 2II,III presents the evolution of Raman oxidation descriptors for trilinolein and trilinolenin, respectively.

The production of allylic radicals by hydrogen abstraction in alpha position (α), relative to the fatty acid chain double bond, is the first step in the oxidation process (Figure 2I.A).^{17,40} This induces a loss in CH_2 numbers and thus the decrease of CH_2 stretching/ CH_3 stretching ratio (Figure 2II.A,III.A). At further steps of oxidation, the decrease is related to the fragmentation of the alkyl chains.

It is worthy to notice the CH_2 stretching/ CH_3 stretching ratio values before irradiation. For trilinolein, the ratio is almost 0.87 (Figure 2II.A) for a $\text{CH}_2/\text{CH}_3 = 12.6$ (38 CH_2 to 3 CH_3). In our previous study, the same ratio (~ 0.87) was obtained for sebaleic acid with a CH_2/CH_3 ratio equal to 12.¹⁷

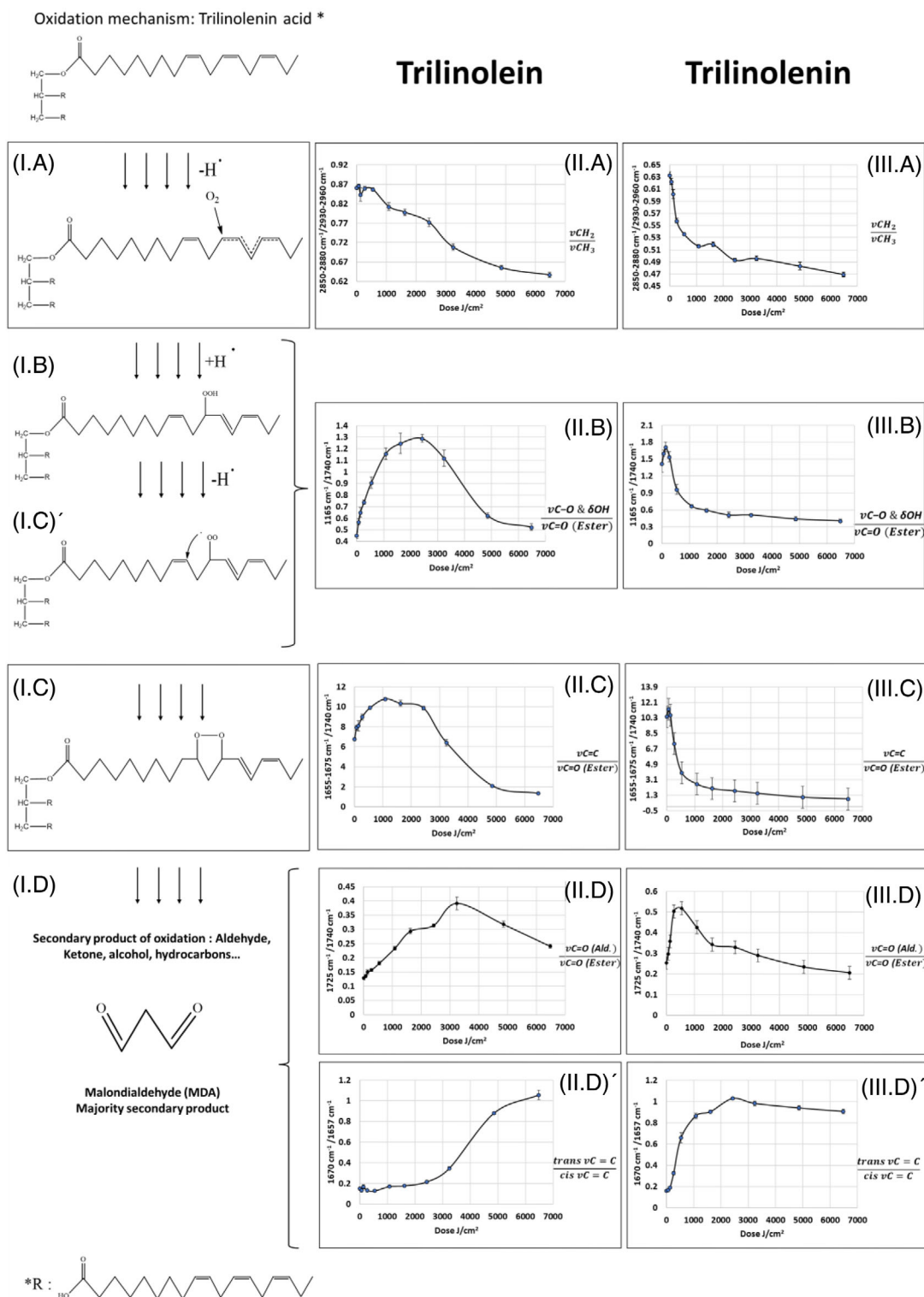


FIGURE 2 (I) Oxidation mechanism of polyunsaturated alkyl chain in triglyceride (TG) (* example of trilinolenin): [(I.A) hydrogen abstraction; (I.B) hydro-peroxidation; (I.B') peroxy radicals formation; (I.C) cyclization; (I.D) formation of secondary oxidation products]. (II) Raman descriptors of trilinolein oxidation. (III) Raman descriptors of trilinolenin descriptors: [(II.A, III.A) CH_2/CH_3 stretching ratio; (II.B, III.B) $\delta(\text{OH})$ and $\nu(\text{C-O})/\nu(\text{C=O})$ (ester) ratio; (II.C, III.C) $\nu(\text{C=C})/\nu(\text{C=O})$ (ester) ratio; (II.D, III.D) $\nu(\text{C=O})$ (aldehyde)/ $\nu(\text{C=C})$ ratio; (II.D', III.D') $\text{trans } \nu(\text{C=C})/\text{cis } \nu(\text{C=C})$ ratio].⁵³⁻⁵⁷

In contrast, for trilinolenin ($\text{CH}_2/\text{CH}_3 = 10.6$ (32 CH_2 to 3 CH_3)) and linolenic acid ($\text{CH}_2/\text{CH}_3 = 10$), the CH_2 stretching/ CH_3 stretching ratio values were 0.63 and 0.72, respectively. The low ratio observed for trilinolenin can be explained by its high auto-oxidation rate. The hydrogen abstraction started before irradiation, and thus, the number of CH_2 was lower.^{46,47}

In the second step, hydroperoxides were produced as primary oxidation products (Figure 2I.B).¹⁷ This can be monitored by following the relative evolution of the band at 1165 cm^{-1} ($\delta(\text{OH})$ bending and $\nu(\text{C}-\text{O})$ stretching). For relative monitoring, this band was divided by the 1740 cm^{-1} band associated with $\nu(\text{C}=\text{O})$ stretching specific to esters. The choice of the 1740 cm^{-1} band as internal standard was related to the fact that the ester function remains intact during the oxidation process.²⁶

For trilinolein, the $1165/1740\text{ cm}^{-1}$ ratio showed an increase from ~ 0.45 before irradiation up to ~ 1.3 after irradiation at 2430 J/cm^2 indicating the formation of hydroperoxides at these doses (Figure 2II.B). After 2430 J/cm^2 , the ratio decreased to reach a plateau at ~ 0.5 . This decrease indicated the fragmentation of hydroperoxides and the formation of higher peroxy radicals.^{17,48} The plateau after 4860 J/cm^2 was at almost the same value before irradiation, which indicated that the observation included the beginning of the formation of hydroperoxides, the increase of their number, then their fragmentation and complete decomposition.

For trilinolenin, the $1165/1740\text{ cm}^{-1}$ ratio was ~ 1.5 before irradiation. It increased up to ~ 1.7 135 J/cm^2 and was followed by a marked decrease to reach a plateau at ~ 0.35 after 1080 J/cm^2 (Figure 2III.B). The high values observed before irradiation were indicative to the presence of hydroperoxides and confirmed the auto-oxidation that was observed by the hydrogen abstraction descriptor. The same information was obtained from the variations in the 1165 cm^{-1} band observed on the Raman spectra plotted in Figure 3A,D.

As described in our previous work on free fatty acids oxidation,¹⁷ hydroperoxides and peroxy radicals are unstable and decompose to a variety of volatile compounds, including aldehydes, ketones, hydrocarbons and other secondary products.⁴⁸

To lead to the formation of these secondary products, a cyclization mechanism (Figure 2I.C) takes place.

The loss of a double bond due to the cyclisation mechanism (Figure 2I.C) can be monitored by the relative evolution of 1675 cm^{-1} ($\nu(\text{C}=\text{C})$). Thus, cyclisation should be related to a decrease in the $1655\text{--}1675/1740\text{ cm}^{-1}$ ($\nu(\text{C}=\text{C})/\nu(\text{C}=\text{O})$ ester) ratio and a decrease in the AUCs of the bands at around 970 cm^{-1} (out of plane vinyl CH bending, $\delta(=\text{CH})$), 1267 cm^{-1} (in plane vinyl CH bending, $\delta(=\text{CH})$) and 3010 cm^{-1} (vinyl CH stretch, $\nu(=\text{CH})$) (Figure 3A,C,D,F).

For trilinolein (Figure 2II.C), an increase was observed from 0 to 1080 J/cm^2 followed by a plateau until 2403 J/cm^2 . At these doses, no modification was observed for the 970 , 1267 and 3012 cm^{-1} bands (Figure 3A,C,D,F). Based on this, the relative increase of the AUC of the 1675 cm^{-1} band cannot be related to variations in the number of double bonds. It can rather be associated with the conjugated double bonds that were generated during the oxidation process (Figure 2I.B,I,B').

After 2403 J/cm^2 , a marked decrease was observed. This decrease can be associated with the loss of double bond and was confirmed by the decrease in the AUC of the out-of-plane vinyl CH bending (970 cm^{-1}), the in-plane vinyl CH bending (1267 cm^{-1}) and the vinyl CH stretch (3010 cm^{-1}) (Figure 3A,C,D,F). It is important to note the parallel evolution between the decomposition of hydroperoxides and peroxy radicals (Figures 2II.B,III.B) and the cyclisation (Figure 2II.C).

Trilinolenin cyclisation (Figure 2III.C) started after 67.5 J/cm^2 . An abrupt decrease of the $\nu(\text{C}=\text{C})/\nu(\text{C}=\text{O})$ ester ratio was observed after 135 J/cm^2 simultaneously with the increase in the hydroperoxidation markers.

In the final steps of the oxidation mechanisms, aldehydes, ketone, alcohols and other secondary products were produced. MDA was described as the major secondary product (Figure 2I.D).¹⁷

The formation of these products can be followed by the evolution of the $1725/1740\text{ cm}^{-1}$ ($\nu(\text{C}=\text{O})$ ald./ $\nu(\text{C}=\text{O})$ ester) ratio. For both TGs, this ratio showed an increase, simultaneously with other oxidation steps. The maximum values were obtained at 3240 and 540 J/cm^2 for trilinolein and trilinolenin, respectively (Figure 2II.D,III.D). After these doses, the balance between the production of the volatile compounds and their evaporation was inverted resulting in a decrease in the ratio values.

Finally, the increase in the *trans* conformers was described by Muik et al. as related to the formation of *trans* secondary oxidation products.²⁶ The *trans* $\nu(\text{C}=\text{C})/\text{cis}$ $\nu(\text{C}=\text{C})$ ratio is presented in Figure 2II.D',III.D'. For trilinolein, a marked increase was observed after 3240 J/cm^2 (Figure 2II.D') with a dose decay compared to the decrease in the global $\nu(\text{C}=\text{C})$ content (Figure 2II.C). The continuous increase of the *trans/cis* ratio was associated with the presence of other *trans* secondary oxidation products than the volatile compounds.

Similar observations were obtained for trilinolenin (Figure 2III.D') with a plateau for higher doses. This was related to the higher oxidation rate of this TG. The conformer changes were also seen by the broadening of the peak at around 1657 cm^{-1} in Raman spectra for both TGs (Figure 3B,E).

In addition to the structural evolution, organizational and conformational changes were observed. Figure 3C,F shows a decrease of the $\nu(\text{CH}_2)$ asym shoulder at around 2870 cm^{-1} indicating higher inter-chain disorder along with irradiation. As mentioned in our previous study, the decrease in the AUC of the 2870 cm^{-1} band may contribute to the observed decrease of the CH_2/CH_3 ratio.¹⁷

4 | CONCLUSION

SSLs and stratum corneum (SC) lipids represent the first barrier protecting our body against external insults. Even though the effect of solar radiations on skin is well documented, their effect on Skin SSLs and SC lipids is generally observed at the end of the oxidation process.^{49–52}

This paper is the second part of a global study that aims to put together different spectral descriptors to follow the different

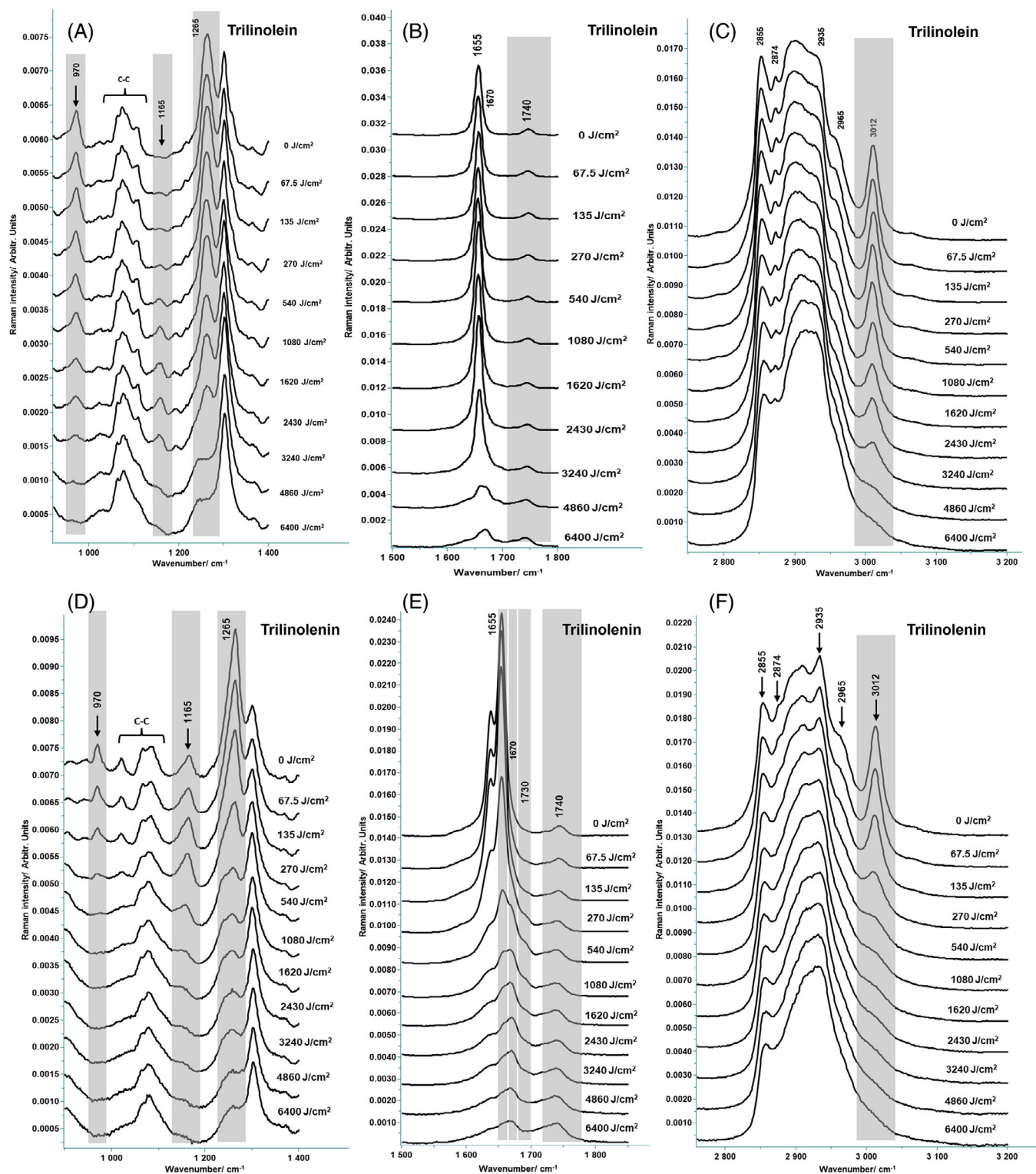


FIGURE 3 (A–F) Raman spectra of trilinolein and trilinolenin at different UV doses.

structural modifications during the photo-oxidation process, that is hydrogen abstraction, formation of hydroperoxides and peroxy radicals as primary oxidation products and the formation of aldehydes, ketones, alcohol as secondary products. In the first part, the use of vibrational spectroscopies enabled to monitor, step by step, the oxida-

tion process of fatty acids induced by different doses of solar radiations obtained under a solar simulator.¹⁷ In this part, the photo-oxidation of five TGs, tripalmitolein, 1,2-palmitolein-3-palmitin and 1,2-palmitin-3-palmitolein, trilinolein and trilinolenin was studied. Saturated and monounsaturated TG were not prone to oxidation. Trilinolein and trili-

nolenin followed an oxidation process similar to sebaleic and linolenic acids with oxidation steps occurring at lower doses.

CONFLICT OF INTEREST STATEMENT

The author declares that there is no conflict of interest.

DATA AVAILABILITY STATEMENT

Data available upon reasonable request.

ORCID

Ali Assi  <https://orcid.org/0000-0002-5019-0100>

REFERENCES

- Correia BSB, Torrinhas RS, Ohashi WY, Tasić L. Analytical tools for lipid assessment in biological assays. *Advances in Lipid Metabolism*. 2018.
- Fahy E, Cotter D, Sud M, Subramaniam S. Lipid classification, structures and tools. *Biochim Biophys Acta*. 2011;1811(11):637.
- Halliwel B, Chirico S. Lipid peroxidation: Its mechanism, measurement, and significance. *Am J Clin Nutr*. 1993;57:715S.
- Mylonas CG, Kouretas D. Lipid peroxidation and tissue damage. *In vivo*. 1999;13(3):295.
- Shichiri M, Yoshida Y, Niki E. In: Watson RR, De Meester F, eds. *Omega-3 Fatty Acids in Brain and Neurological Health*. Academic Press; 2014:31.
- Spiteller G. Linoleic acid peroxidation—the dominant lipid peroxidation process in low density lipoprotein—and its relationship to chronic diseases. *Chem Phys Lipids*. 1998;95:105.
- Sjövall P, Skedung L, Gregoire S, Biganska O, Clément F, Luengo GS. Imaging the distribution of skin lipids and topically applied compounds in human skin using mass spectrometry. *Sci Rep*. 2018;8:16683.
- Lasch J, Schonfelder U, Walke M, Zellmer S, Beckert D. Oxidative damage of human skin lipids. *Biochim Biophys Acta*. 1997;1349:171.
- Niki E. Role of vitamin E as a lipid-soluble peroxy radical scavenger: In vitro and in vivo evidence. *Free Radic Res*. 2014;49:1.
- Niki E. Lipid oxidation in the skin. *Free Radical Res*. 2015;49:827.
- Rajneesh CP, Manimaran A, Sasikala KR, Adaikappan P. Lipid peroxidation and antioxidant status in patients with breast cancer. *Singapore Med J*. 2008;49(8):640.
- Esterbauer H, Wäg G, Puhl H. Lipid peroxidation and its role in atherosclerosis. *British Medical Bulletin*. 1993;49(3):566.
- Kabir T, Rahman H, Shah M, et al. Therapeutic promise of carotenoids as antioxidants and anti-inflammatory agents in neurodegenerative disorders. *Biomedicine Pharmacotherapy*. 2022;146:112610.
- Ferré-González L, Peña-Bautista C, Baquero M, Cháfer-Pericás C. Assessment of lipid peroxidation in Alzheimer's disease differential diagnosis and prognosis. *Antioxidants*. 2022;11:551.
- Catala A, Diaz M. Editorial: impact of lipid peroxidation on the physiology and pathophysiology of cell membranes. *Front Physiol*. 2016;7:423.
- Spickett CM. The lipid peroxidation product 4-hydroxy-2-nonenal: advances in chemistry and analysis. *Redox Biol*. 2013;1:145.
- Assi A, Michael-Jubeli R, Baillet-Guffroy A, Tfayli A. Skin surface lipids photo-oxidation: A vibrational spectroscopy study. *J Raman Spectrosc*. 2023.
- Sylvie E. *Ecole polytechnique de l'Université de Nantes*. PhD thesis. France; 2003.
- Kim EJ, Jin XJ, Kim YK, et al. UV decreases the synthesis of free fatty acids and triglycerides in the epidermis of human skin in vivo, contributing to development of skin photoaging. *J Dermatol Sci*. 2010;57:19.
- Karatas F, Karatepe M, Baysar A. Determination of free malondialdehyde in human serum by high-performance liquid chromatography. *Anal Biochem*. 2002;311:76.
- Zelzer S, Oberreither R, Bernecker C, Stelzer I, Truschig-Wilders M, Fauler G. Oxidative stress: Determination of 4-hydroxy-2-nonenal by gas chromatography/mass spectrometry in human and rat plasma. *Free Radical Res*. 2013;49(10):1233.
- Young IS, Trimble ER. Measurement of malondialdehyde in plasma by high performance liquid chromatography with fluorimetric detection. *Ann Clin Biochem*. 1991;28(pt 5):504.
- Dong X, Tang J, Chen X. Sensitive determination of malondialdehyde in rat prostate by high performance liquid chromatography with fluorescence detection. *Sci Rep*. 2020;10:3990.
- Ma L, Liu G. Simultaneous analysis of malondialdehyde, 4-hydroxy-2-hexenal, and 4-hydroxy-2-nonenal in vegetable oil by reversed-phase high-performance liquid chromatography. *J Agric Food Chem*. 2017;65:11320.
- Yonny ME, Rodríguez Torressi A, Nazareno MA, Cerutti S. Development of a novel, sensitive, selective, and fast methodology to determine malondialdehyde in leaves of melon plants by ultra-high-performance liquid chromatography-tandem mass spectrometry. *J Anal Methods Chem*. 2017;2017:4327954.
- Muik B, Lendl B, Molina-Díaz A, Ayora-Cañada MJ. Direct monitoring of lipid oxidation in edible oils by Fourier transform Raman spectroscopy. *Chem Phys Lipids*. 2005;134:173.
- Machado NFL, de Carvalho LAEB, Otero JC, Marques MPM. The autooxidation process in linoleic acid screened by Raman spectroscopy. *J Raman Spectrosc*. 2012;43:1991.
- Guillén MD, Cabo N. Usefulness of the frequency data of the Fourier transform infrared spectra to evaluate the degree of oxidation of edible oils. *J Agric Food Chem*. 1999;47:709.
- Agbenyega JK, Claybourn M, Ellis G. A study of the autoxidation of some unsaturated fatty acid methyl esters using Fourier transform Raman spectroscopy. *Spectrochim Acta A: Mol Spectrosc*. 1991;47:1375.
- Czamara K, Majzner K, Pacia MZ, Kochan K, Kaczor A, Baranska M. Raman spectroscopy of lipids: a review. *J Raman Spectrosc*. 2015;46:4.
- Gang L, Guoping Z. Raman spectroscopy application to analyses of components in aqueous solutions. *ProcSPIE*. 2006;6047:60472V.
- Li N, Sancak Y, Frasar J, Atilla-Gokcumen GA-O. A Protective Role for Triacylglycerols during Apoptosis. *Biochemistry*. 2017;57(1):72.
- Yen C-LE, Stone SJ, Koliwad S, Harris C, Farese RV Jr. Thematic review series: Glycerolipids. DGAT enzymes and triacylglycerol biosynthesis. *J Lipid Research*. 2008;49(11):2283.
- Coleman RA, Mashek DG. Mammalian triacylglycerol metabolism: Synthesis, lipolysis, and signaling. *Chem Rev*. 2011;111(10):6359.
- Lieber CA, Majumder SK, Ellis DL, Billheimer DD, Mahadevan-Jansen A. In vivo nonmelanoma skin cancer diagnosis using Raman microspectroscopy. *Lasers Surg Med*. 2008;40(7):461.
- Rael L, Thomas G, Craun M, Curtis C. Lipid peroxidation and the thiobarbituric acid assay: Standardization of the assay when using saturated and unsaturated fatty acids. *J Biochem Mol Biol*. 2004;37:749.
- Tfayli A, Guillard E, Manfait M, Baillet-Guffroy A. Thermal dependence of Raman descriptors of ceramides. Part I: Effect of double bonds in hydrocarbon chains. *Anal Bioanal Chem*. 2010;397:1281.
- Guillard E, Tfayli A, Manfait M, Baillet-Guffroy A. Thermal dependence of Raman descriptors of ceramides. Part II: Effect of chains lengths and head group structures. *Anal Bioanal Chem*. 2011;399:1201.
- Bresson S, Marssi ME, Khelifa B. Raman spectroscopy investigation of various saturated monoacid triglycerides. *Chem Phys Lipids*. 2005;134:119.
- Frankel EN. Chemistry of free radical and singlet oxidation of lipids. *Prog Lipid Res*. 1984;23:197.
- Shah D, Mahajan N, Sah S, Nath SK, Paudyal B. Oxidative stress and its biomarkers in systemic lupus erythematosus. *J Biomed Sci*. 2014;21:23.
- Niki E. Lipid peroxidation: physiological levels and dual biological effects. *Free Radic Biol Med*. 2009;47:469.
- Girotti AW. Mechanisms of lipid peroxidation. *J Free Radic Biol Med*. 1985;1:87.

44. Porter NA, Caldwell SE, Mills KA. Mechanisms of free radical oxidation of unsaturated lipids. *Lipids*. 1995;30:277.
45. Michel F, Bonnefont-Rousselot D, Mas E, Draï J, Thérond P. Biomarkers of lipid peroxidation: Analytical aspects. *Ann Biol Clin*. 2008;66:605.
46. Orlova Y, Harmon RE, Broadbelt LJ, Iedema PD. Review of the kinetics and simulations of linseed oil autoxidation. *Prog Org Coat*. 2021;151:106041.
47. Marshall GL. The analysis of cured drying oils by swollen state ¹³C-NMR spectroscopy. *Eur Polym J*. 1986;22:231.
48. Cao J, Deng L, Zhu XM, et al. Novel approach to evaluate the oxidation state of vegetable oils using characteristic oxidation indicators. *J Agric Food Chem*. 2014;62:12545.
49. Trommer H. The examination of skin lipid model systems stressed by ultraviolet irradiation in the presence of transition metal ions. *Eur J Pharm Biopharm*. 2001;51:207.
50. Trommer H, Bottcher R, Poppl A, Hoentsch J, Wartewig S, Neubert RH. Role of ascorbic acid in stratum corneum lipid models exposed to UV irradiation. *Pharm Res*. 2002;19:982.
51. Merle C, Laugel C, Baillet-Guffroy A. Spectral monitoring of photoirradiated skin lipids: MS and IR approaches. *Chem Phys Lipids*. 2008;154:56.
52. Merle C, Laugel C, Baillet-Guffroy A. Effect of UVA or UVB irradiation on cutaneous lipids in films or in solution. *Photochem Photobiol*. 2010;86:553.
53. Larsson K. Conformation-dependent features in the Raman spectra of simple lipids. *Chem Phys Lipids*. 1973;10:165.
54. Verma SP, Wallach DFH. Raman spectra of some saturated, unsaturated and deuterated C18 fatty acids in the HCH-deformation and CH-stretching regions. *Biochim Biophys Acta (BBA) - Lipids Lipid Metab*. 1977;486:217.
55. Wegener M, Neubert R, Rettig W, Wartewig S. Structure of stratum corneum lipids characterized by FT-Raman spectroscopy and DSC. I. Ceramides. *Int J Pharm*. 1996;128:203.
56. Frankel EN. Chemistry of free radical and singlet oxidation of lipids. *Prog Lipid Res*. 1984;23:197.
57. Shah D, Mahajan N, Sah S, Nath SK, Paudyal B. Oxidative stress and its biomarkers in systemic lupus erythematosus. *J Biomed Sci*. 2014;21:23.

How to cite this article: Assi A, Michael-Jubeli R, Jacques-Jamin C, Baillet-Guffroy A, Duplan H, Tfyayli A. Characterization of triglycerides photooxidation under solar radiations: A stepwise Raman study. *Anal Sci Adv*. 2023;4:293–301. <https://doi.org/10.1002/ansa.202200060>